

Structurally frustrated polar nanoregions in BaTiO₃-based relaxor ferroelectric systems

Y. Liu,^{a)} R. L. Withers, and B. Nguyen

Research School of Chemistry, The Australian National University, Canberra, Australian Capital Territory 0200, Australia

K. Elliott

Research School of Chemistry and Faculty of Engineering and Information Technology, The Australian National University, Canberra, Australian Capital Territory 0200, Australia

(Received 31 July 2007; accepted 7 September 2007; published online 11 October 2007)

This letter presents direct electron diffraction evidence that structurally frustrated one-dimensional polar nanoregions arising from anticorrelated displacements of Ti and nearest neighboring O ions are responsible for the relaxation behavior observed in doped BaTiO₃ relaxor ferroelectrics, rather than chemical short range ordering. The role of the dopant ions is not to directly induce polar nanoregions but rather to set up random local strain fields preventing homogeneous strain distortion, thereby suppressing transverse correlation from one $\langle 001 \rangle$ chain dipole to the next and hence the development of long range ferroelectric order. © 2007 American Institute of Physics.

[DOI: 10.1063/1.2790481]

BaTiO₃-doped relaxor ferroelectrics are characterized by broad frequency dispersive dielectric constant maxima at a “diffuse phase transition” temperature T_m , a slim P - E ferroelectric hysteresis loop, and ideal, cubic perovskite, average structures both above and below T_m . They continue to be widely studied for their potential applications as lead-free, electrostrictive, and/or piezoelectric sensors and actuators as well as for the electrical field tunability of their dielectric properties.^{1–3} Relaxor ferroelectric behavior of the above type has long been attributed to the existence of so-called polar nanoregions (PNRs).^{4–7} The precise nature of these PNRs and their relationship to the compositional heterogeneity [sometimes called chemical nanoregions⁷ (CNRs)] characteristic of all relaxor ferroelectrics, however, is still far from well understood. Because compositional heterogeneity has been shown to be essential for the observation of relaxor ferroelectric properties in disordered perovskites such as Pb(Sc_{0.5}Ta_{0.5})O₃,⁵ it is often assumed that PNRs are not an inherent feature of such materials but rather are somehow induced by, and directly coupled to, the compositional heterogeneity, i.e., to the CNRs.

Other authors,^{7,8} on the basis of broadband dielectric spectroscopy⁸ coupled with the reasonable assumption that compositional disorder is necessarily frozen up until very high temperature and hence not available to couple directly to the much lower temperature dynamical disorder associated with the dielectric relaxation properties of relaxor ferroelectrics, suggest that PNRs cannot therefore be directly coupled to the CNRs. Rather, these authors argue that the PNRs arise from inherent dynamical disorder associated with the motion of correlated clusters of atoms (dynamic above T_m and frozen in below T_m)—in the case of Pb-containing perovskites, for example, caused by the inherent anharmonic motion of correlated clusters of Pb ions.⁸ We have recently observed similar behavior in the case of the Ba(Ti_{1-x}Sn_x)O₃ system⁹ by means of electron diffraction. In this case, the equivalent inherent dynamic disorder is associated with anharmonic

motion of $\langle 001 \rangle$ correlated clusters of Ti and neighboring O ions. This has prompted a further investigation of other doped BaTiO₃ relaxor ferroelectric systems to see if such behavior is universal.

The typical BaTiO₃-doped relaxor ferroelectrics Ba(Ti_{0.7}Zr_{0.3})O₃ (BTZ), Ba(Ti_{0.7}Sn_{0.3})O₃ (BTSn), Ba_{0.925}(Ti_{0.85}Nb_{0.15})O₃ (BTN), and (Ba_{0.75}Sr_{0.25})TiO₃ (BSrT) were thus synthesized by solid state reaction using high purity BaCO₃, SrCO₃, and related oxides (SnO₂, TiO₂, ZrO₂, and Nb₂O₅). The resultant samples had metrically cubic lattice parameters of $a=4.0597(4)$ Å (BTZ), 4.0401(6) Å (BTSn), 4.0199(7) Å (BTN), and 3.9764(6) Å (BSrT). The relative density of all pellets was >95% while the average grain size was ~5–10 μm.

The dopant level in each case is sufficiently high that all four compounds exhibit characteristic relaxor ferroelectric behavior^{9–13} with the diffuse phase transition at T_m , corresponding to the peak of the permittivity as a function of temperature, occurring below room temperature.^{9–13} Thus, the dipole dynamics associated with the PNRs are yet to freeze in⁷ at room temperature and hence direct transmission electron microscope (TEM) imaging is not an appropriate tool (the exposure time for such an image is >~1 s) to look for evidence of dynamic PNRs.¹⁴ For the same reason, other imaging techniques such as piezoresponse force microscopy,¹⁵ are also not appropriate tools to look for evidence of dynamic PNRs. Electron diffraction, on the other hand, is known to be sensitive to dynamical displacive disorder¹⁶ and was thus used to look for evidence of the dynamic PNRs (and static CNRs).

Figure 1 shows typical (a) $[-1, 2, 0]$ and (b) $[-1, 4, 0]$ zone axis electronic diffraction patterns (EDPs) of BTZ, (c) a $[-1, 2, 0]$ zone axis EDPs of BTSn, (d) a $[-1, 4, 0]$ zone axis EDP of BSrT, and (e) $\sim[-1, 2, 0]$ and (f) $[-1, 4, 0]$ zone axis EDPs of BTN. Note the characteristic diffuse streaking always perpendicular to $\langle 001 \rangle$ real space directions in these EDPs, e.g., along $\langle 210 \rangle^*$, $\langle 410 \rangle^*$, $\langle 001 \rangle^*$ in Fig. 1 running through all parent perovskite Bragg reflections \mathbf{G} and together forming $\{001\}^*$ sheets of diffuse intensity. $\{001\}^*$

^{a)}Electronic mail: yliu@rsc.anu.edu.au

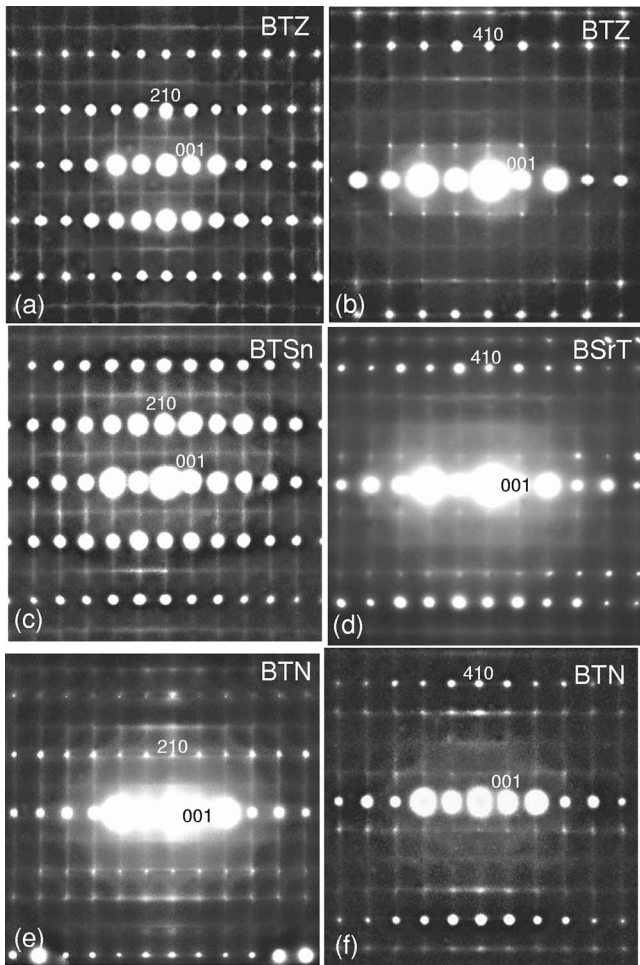


FIG. 1. Typical (a) $[-1, 2, 0]$ and (b) $[-1, 4, 0]$ zone axis EDPs of BTZ, (c) $[-1, 2, 0]$ zone axis EDP of BTSn, (d) $[-1, 4, 0]$ zone axis EDP of BSrT, and (e) $\sim[-1, 2, 0]$ and (f) $[-1, 4, 0]$ zone axis EDPs of BTN.

sheets of diffuse intensity in reciprocal space imply one-dimensional (1D) $\langle 001 \rangle$ columns of correlated atom displacements in real space. Very similar, relatively sharp, transverse polarized,¹⁶ $\{001\}^*$ sheets of diffuse intensity were observed for each of the four BZT, BNT, BSrT, and BTSn samples. Essentially identical diffuse scattering¹⁷⁻¹⁹ was long ago reported to be characteristic of the undoped end-member compound BaTiO_3 and also shown to be closely associated with the paraelectric to tetragonal ferroelectric and subsequent phase transitions thereof. This strongly suggests that the observed diffuse distributions and hence the 1D PNRs (see below) in the doped BaTiO_3 relaxor ferroelectrics are not induced by the dopant ions but rather are an inherent characteristic of the end-member BaTiO_3 compound itself.

Note that the zero magnitude component of the individual $\mathbf{q} = \langle hk0 \rangle^*$, h, k continuous, modulation wave vectors constituting the individual $\{001\}^*$ sheets of diffuse intensity along the orthogonal $\langle 001 \rangle$ real space directions regardless of the Ti/Zr, Ti/Sn, Ti/Nb, and Ba/Sr composition ratios rules out the possibility of Ti/Zr, Ti/Sn, Ti/Nb, and Ba/Sr compositional orderings being directly responsible for the observed diffuse distribution.^{9,20} Nonetheless, it is possible to envisage $\langle 001 \rangle$ strings of \cdots -dopant-O-dopant- \cdots ions along the $\langle 001 \rangle$ directions embedded in much longer strings of \cdots -Ti-O-Ti- \cdots ions which might be compatible with the observed diffuse distribution. The length of these \cdots -dopant-O-dopant- \cdots strings, however, would need to be quite long

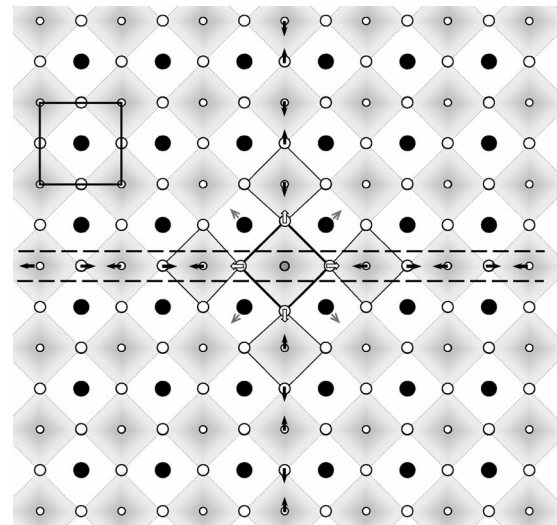


FIG. 2. An instantaneous snapshot in projection along an $\langle 001 \rangle$ direction showing the 1D PNRs implied by the observed electron diffraction evidence characteristic of all four BaTiO_3 -doped relaxor ferroelectrics. The oppositely directed shifts along $\langle 100 \rangle$ of neighboring Ti and O ions are labeled by arrows. This leads to the formation of 1D polarization along the $\langle 001 \rangle$ direction (see between the two dashed lines). The Ba, Ti, O, and dopant M ions are represented by the black solid circles, the small open circles, the big open circles, and the gray solid circles, respectively. The average structure unit cell is marked by a square in the top left hand corner.

($> \sim 5-10$ unit cells), otherwise the relatively sharp $\{001\}^*$ sheets of diffuse intensity would be streaked out not only perpendicular to $\langle 001 \rangle^*$ but also along $\langle 001 \rangle^*$ (see, e.g., Refs. 19 and 21). Note that there is some evidence from extended x-ray-absorption fine structure²² and high pressure Raman²³ investigations of BTZ for clustering of the Zr ions.

The transverse polarized^{9,16} nature of the characteristic diffuse distribution is clear from its strong azimuthal intensity variation and shows that the observed $\{001\}^*$ sheets of diffuse intensity arise from correlated longitudinal motions of ions along the $\langle 001 \rangle$ real space directions.

Furthermore, the characteristic variation in diffuse intensity from one $\mathbf{G} \pm \{001\}^*$ sheet to the next (being careful to avoid the distorting effect of multiple scattering),¹⁶ shows that the individual $\mathbf{q} = \langle 0kl \rangle^*$ modes of distortion responsible for the observed diffuse scattering are inherently polar, or transverse optical (TO) type, in nature, e.g., the $h/4\langle 410 \rangle^* + \gamma\langle 001 \rangle^*$, h odd, diffuse streaking in Figs. 1(b), 1(d), and 1(f) is always considerably more intense than the h even diffuse streaking while the $h/2\langle 210 \rangle^* + \gamma\langle 001 \rangle^*$, h odd, diffuse streaking in Figs. 1(a), 1(c), and 1(e) is always considerably more intense than the h even diffuse streaking. This requires that the Ti ion at 000 and the O ion above it at $\frac{1}{2}, 0, 0$ (along the polar $\langle 100 \rangle$ directions) necessarily shift in opposite directions along $\langle 100 \rangle$ for all \mathbf{q} , as shown schematically in Fig. 2, see Ref. 9 for more details. (Such a displacement eigenvector is not compatible with an interpretation of the observed diffuse in terms of relatively long $\langle 001 \rangle \cdots$ dopant-O-dopant- \cdots ion strings and associated structural relaxation, see above.) Note that by TO type above, we are referring to the necessarily oppositely directed character of the $\langle 100 \rangle$ shifts of the Ti and O ions and not to any characteristic time scale associated with the correlated simultaneous flipping of the displacements associated with these 1D PNRs. The latter dynamic character to the existence of these PNRs is shown by the broadband dielectric spectroscopy

results⁸ but does not affect the above diffraction results.

The diffraction evidence thus clearly demonstrates extremely anisotropic, anticorrelated behavior of the off-center displacements of the Ti and O ions ultimately responsible for the observed dielectric relaxation behavior of BTZ, BTSn, BTN, and BSrT. That the observed diffuse scattering exists above T_m in all four cases requires that the 1D PNRs also continue to exist above the diffuse phase transition at T_m ,⁹ which in turn suggests that the diffuse phase transition can only be due to the low temperature freezing in of their dipole dynamics.⁷ As mentioned above, the same highly correlated, anisotropic $\langle 001 \rangle$ chain dipoles (PNRs) are also known to be characteristic of the paraelectric phase of the end-member BaTiO₃ itself^{17–19} and induced by covalent hybridization between Ti d and O $2p$ orbitals^{24–27} along the $\langle 001 \rangle$ real space directions. The existence of the 1D $\langle 001 \rangle$ PNRs implied by the $\{001\}^*$ sheets of diffuse intensity in these BaTiO₃ doped relaxor ferroelectric materials thus have nothing directly to do with the doping level, or with CNRs in general, but rather are intrinsic to the end-member BaTiO₃ itself^{24–26} or, more correctly, to covalent hybridization between Ti d and O $2p$ orbitals^{24–27} along the $\langle 001 \rangle$ real space directions.

BaTiO₃ itself, however, does not exhibit relaxor ferroelectric behavior. If the doping does not locally induce the PNRs, then what is the role of the chemical disorder? We suggest that the role of the dopant ions is to set up random local strain fields suppressing transverse correlations of the $\langle 001 \rangle$ chain dipoles and the development of long range ordered ferroelectric state/s below T_m . Theoretical calculations have shown that homogeneous strain distortion plays a critical role in the stabilization of the low temperature ferroelectric phases of BaTiO₃.^{24–27} It would not then be surprising if essentially random local strain distortions induced by doping would suppress the condensation of long wavelength homogeneous strain distortions of the unit cell, thereby suppressing transverse correlations of the $\langle 001 \rangle$ chain dipoles and the development of long range ordered ferroelectric state/s below T_m .

Given that 1D PNRs are an inherent feature of BaTiO₃ itself, it is perhaps not surprising that neither homovalent nor heterovalent substitution onto the perovskite B (or Ti) site has a drastic effect on the formation of the 1D PNRs themselves. The level and type of doping clearly do, however, affect the PNR dipole dynamics. Thus, Ba(Ti_{1-x}Zr_x)O₃ does not exhibit clear relaxor ferroelectric behavior until $x > \sim 0.27$ (Ref. 10) and Ba(Ti_{1-x}Sn_x)O₃ until $x > \sim 0.20$,⁹ while Ba_{1-x/2}(Ti_{1-x}Nb_x)O₃ exhibits such behavior at a much lower dopant level ~ 0.06 .¹¹ Likewise, the freezing in of the dipole dynamics, as reflected in the value of T_m , is also strongly affected by the level and type of doping. Thus, T_m in the case of BTN with $x=0.15$ declines rapidly to ~ 100 K, much lower than that observed for both BTSn and BTZ with similar values of x . From Fig. 1(d), even significant Sr doping onto the perovskite A site does not destroy the 1D PNRs although the relative intensity of the diffuse streaking in this case appears to be weaker and less sharp than in the three other doped samples.

The sharpness of the diffuse streaking in Fig. 1 suggests that the dopant ions do not significantly disrupt the longitudinal correlation length along the $\langle 001 \rangle$ dipole chains. The complete disappearance of the paraelectric cubic to tetragonal ferroelectric (and other subsequent) phase transitions in

BaTiO₃, however, strongly suggests that the role of the dopant ions is to frustrate transverse correlation from one such dipole chain to the next and hence to prevent the condensation of a long range ordered ferroelectric state.

In summary, direct evidence for 1D PNRs has been observed in four different types of doped BaTiO₃ relaxor ferroelectric compounds in the form of $\{001\}^*$ sheets of diffuse intensity running through all parent perovskite Bragg reflections \mathbf{G} . A characteristic variation in diffuse intensity from one $\mathbf{G} \pm \{001\}^*$ sheet to the next shows that the 1D $\langle 001 \rangle$ atom displacements responsible are inherently polar in nature and cannot be associated with CNRs. These 1D PNRs are correlated along the $\langle 001 \rangle$ column directions but without any lateral correlation from one such column to the next. The role of the dopant ions appears to be to set up random local strain fields suppressing transverse correlations of these $\langle 001 \rangle$ chain dipoles and frustrating the development of long range ferroelectric order. Nonetheless, below the freezing temperature of the dipole dynamics, the application of a sufficiently large applied electric field can align these 1D PNRs.

Y.L., R.L.W., and B.N. acknowledge financial support from the Australian Research Council (ARC) in the form of an ARC Discovery Grant.

¹J. Cieminski and H. Beige, J. Phys. D **24**, 1182 (1991).

²W. Kleemann, J. Mater. Sci. **41**, 129 (2006).

³K. Uchino, Ferroelectrics **151**, 321 (1994).

⁴G. A. Smolenskii, A. I. Agranovskaya, Sov. Phys. Solid State **1**, 1429 (1959).

⁵L. E. Cross, Ferroelectrics **76**, 241 (1987).

⁶G. A. Samara, J. Phys.: Condens. Matter **15**, R367 (2003).

⁷A. A. Bokov and Z.-G. Ye, J. Mater. Sci. **41**, 31 (2006).

⁸V. Bovtun, J. Petzelt, V. Porokhonsky, S. Kamba, and Y. Yakimenko, J. Eur. Ceram. Soc. **21**, 1307 (2001).

⁹Y. Liu, R. L. Withers, X. Wei, and J. D. Fitz Gerald, J. Solid State Chem. **180**, 858 (2007).

¹⁰R. Farhi, M. El Marssi, A. Simon, A. Simon, and J. Ravez, Eur. Phys. J. B **9**, 599 (1999).

¹¹R. Farhi, M. El Marssi, A. Simon, and J. Ravez, Eur. Phys. J. B **18**, 605 (2000).

¹²R. Zhang, J. F. Li, and D. Viehland, Ferroelectr., Lett. Sect. **29**, 125 (2002).

¹³H. V. Alexandru, C. Berbecaru, A. Ioachim, M. I. Toacsen, M. G. Banciu, L. Nedelcu, and D. Ghetu, Mater. Sci. Eng., B **109**, 152 (2004).

¹⁴G. van Tendeloo and S. Amelinckx, Phase Transitions **67**, 101 (1998).

¹⁵V. V. Shvartsman, W. Kleemann, J. Dec, Z. K. Xu, and S. G. Lu, J. Appl. Phys. **99**, 124111 (2006).

¹⁶R. L. Withers, Z. Kristallogr. **220**, 1027 (2005).

¹⁷R. Comes, M. Lambert, and A. Guinier, Solid State Commun. **6**, 715 (1968).

¹⁸M. Lambert and R. Comes, Solid State Commun. **7**, 305 (1969).

¹⁹J. Harada, M. Watanabe, S. Kodera, and G. Honjo, J. Phys. Soc. Jpn. **20**, 630 (1965).

²⁰F. J. Brink, L. Norén, and R. L. Withers, J. Solid State Chem. **155**, 2177 (2004).

²¹L. Norén, R. L. Withers, and F. J. Brink, J. Solid State Chem. **178**, 2133 (2005).

²²C. Laulhé, F. Hippert, J. Kreisel, M. Maglione, A. Simon, J. L. Hazemann, and V. Nassif, Phys. Rev. B **74**, 041016 (2006).

²³J. Kreisel, P. Bouvier, M. Maglione, B. Dkhil, and A. Simon, Phys. Rev. B **69**, 092104 (2004).

²⁴R. E. Cohen and H. Krakauer, Phys. Rev. B **42**, 6416 (1990).

²⁵Ph. Ghosez, X. Gonze, and J.-P. Michenaud, Ferroelectrics **206-207**, 205 (1998).

²⁶H. Krakauer, R. Yu, C.-Z. Wang, K. M. Rabe, and U. V. Waghmare, J. Phys.: Condens. Matter **11**, 3779 (1999).

²⁷W. Zhong, D. Vanderbilt, and K. M. Rabe, Phys. Rev. Lett. **73**, 1861 (1994).